LETTERS

Oxidation state of iron in komatiitic melt inclusions indicates hot Archaean mantle

Andrew J. Berry[1], Leonid V. Danyushevsky[2], Hugh St C. O'Neill[3], Matt Newville[4] & Stephen R. Sutton[4,5]

Komatiites are volcanic rocks mainly of Archaean age that formed by unusually high degrees of melting of mantle peridotite. Their origin is controversial and has been attributed to either anhydrous melting of anomalously hot mantle[1–3] or hydrous melting at temperatures only modestly greater than those found today[4,5]. Here we determine the original $Fe^{3+}/\Sigma Fe$ ratio of 2.7-Gyr-old komatiitic magma from Belingwe, Zimbabwe[6], preserved as melt inclusions in olivine, to be 0.10 ± 0.02, using iron K-edge X-ray absorption near-edge structure spectroscopy. This value is consistent with near-anhydrous melting of a source with a similar oxidation state to the source of present-day mid-ocean-ridge basalt. Furthermore, this low $Fe^{3+}/\Sigma Fe$ value, together with a water content of only 0.2–0.3 wt% (ref. 7), excludes the possibility that the trapped melt contained significantly more water that was subsequently lost from the inclusions by reduction to H_2 and diffusion. Loss of only 1.5 wt% water by this mechanism would have resulted in complete oxidation of iron (that is, the $Fe^{3+}/\Sigma Fe$ ratio would be ~1). There is also no petrographic evidence for the loss of molecular water. Our results support the identification of the Belingwe komatiite as a product of high mantle temperatures (~1,700 °C), rather than melting under hydrous conditions (3–5-wt% water), confirming the existence of anomalously hot mantle in the Archaean era.

The oxidation state of a magma is given by the ratio of Fe^{3+} to Fe^{2+} (conveniently expressed as $Fe^{3+}/\Sigma Fe$), and reflects the nature of the source and partial melting conditions[8]. $Fe^{3+}/\Sigma Fe$ affects melt structure, viscosity and the temperature and composition of crystallizing phases. It also affects the speciation and amount of volatiles degassed during volcanic eruptions—particularly sulphur-bearing gases such as SO_2—and, thus, volcanogenic forcing of global climate[9]. However, the final oxidation state measured in an igneous rock reflects not only that of the parental magma but also the influence of many subsequent processes, including degassing at the Earth's surface, alteration and metamorphism. Inclusions of melt trapped in early-crystallizing minerals such as olivine potentially preserve nearly pristine, pre-eruptive, undegassed samples of the magma, but the typically small size of such inclusions (<50 μm) has hitherto precluded the precise determination of $Fe^{3+}/\Sigma Fe$. Here we accurately obtain $Fe^{3+}/\Sigma Fe$ from individual melt inclusions.

$Fe^{3+}/\Sigma Fe$ in silicate glasses can be determined by redox titrations, commonly referred to as 'wet chemistry'[10,11], and Mössbauer spectroscopy[12], but these methods lack spatial resolution and are generally restricted to bulk samples. Electron energy-loss spectroscopy[13] and the electron microprobe[14] have the spatial resolution desired, but the techniques are unlikely to be suitable for the analysis of glass inclusions, owing to the high electron beam fluxes involved and the likelihood of beam-induced changes in oxidation state occurring. X-ray absorption near-edge structure (XANES) spectroscopy, which has micrometre spatial resolution, is non-destructive, element specific and requires no sample preparation other than a polished surface, has promised much for a number of years[15], but accurate quantification of $Fe^{3+}/\Sigma Fe$ has been hindered by the need for compositionally matched standards and a lack of sufficient precision in the limited $Fe^{3+}/\Sigma Fe$ range of most terrestrial samples[15–17]. However, it has been shown recently that oxidation state ratios in glasses can be determined with great accuracy and precision, by preparing a series of standards as a function of oxygen fugacity (f_{O_2}) that allows $M^{n+}/\Sigma M$ (for an element M with oxidation state $n+$) to be systematically varied in a way that is generally not possible for minerals, owing to the constraints of crystal chemistry[18,19].

The preparation of glass standards of mid-ocean-ridge basalt (MORB), tholeiite, pantellerite and andesite compositions, and the acquisition of XANES spectra are described in the Methods. XANES spectra for the MORB standard glasses are shown in Fig. 1a. The spectra comprise an absorption edge and a pre-edge feature corresponding to the $1s \rightarrow 3d$ transition. This feature, which is shown in detail in Fig. 1b, comprises transitions to the crystal field levels of Fe^{2+} and Fe^{3+} in the various coordination environments present in the glass[20]. It is possible to reproduce the pre-edge by quantitatively modelling these transitions, using a line shape predicted from the instrumental (Gaussian) and electronic (Lorentzian) contributions to the spectral resolution, but this is unnecessary for quantifying the $Fe^{3+}/\Sigma Fe$ ratio. Instead, as seen in Fig. 1b, the feature shifts to higher energy with increasing oxidation state, owing to the change in energy of the final crystal field levels, allowing an empirical calibration curve to be constructed; the transition intensity changes with the site symmetry[18,21,22].

The key to determining the pre-edge energy precisely is deconvolution from the absorption-edge baseline. Here the pre-edge was fit to two pseudo-Voigt peaks, constrained to have the same width and line shape, simultaneously with the baseline, which was modelled as the tail of two other pseudo-Voigt functions. An example fit is shown in Fig. 1c. The intensity-weighted energy, or centroid, of the baseline-subtracted pre-edge can then be correlated with the $Fe^{3+}/\Sigma Fe$ value of the standards. The resulting calibration curve, obtained using all the compositions studied, is shown in Fig. 2. The functional form of the calibration may vary with the method used to model the baseline; what is important for accurate and precise $Fe^{3+}/\Sigma Fe$ determinations is that the standards and unknown contain iron at similar sites (which is assumed for similar compositions cooled at similar rates) and that all spectra are processed identically.

The validity of the approach was tested by determining $Fe^{3+}/\Sigma Fe$ for a number of olivine-hosted MORB melt inclusions. The inclusions were rapidly heated (to 1,250 °C in 5 min) and quenched to produce a glass. The similar heating and quenching paths of both the unknown and the standard should produce similar iron coordination environments, thus allowing quantification of the unknown from the

[1]Department of Earth Science and Engineering, Imperial College London, South Kensington, SW7 2AZ, UK. [2]CODES, University of Tasmania, Hobart, Tasmania 7001, Australia. [3]Research School of Earth Sciences, Australian National University, Canberra, ACT 0200, Australia. [4]Center for Advanced Radiation Sources, [5]Department of Geophysical Sciences, University of Chicago, Chicago, Illinois 60637, USA.

standard calibration curve. The average $Fe^{3+}/\Sigma Fe$ for the MORB inclusions using the calibration shown in Fig. 2 was 0.14 ± 0.03, in excellent agreement with the value of 0.13 ± 0.02 determined by wet chemical analysis in ref. 11, where it was also found that the f_{O_2} of MORB does not vary between oceanic settings or enriched or depleted melts. This constant value of $Fe^{3+}/\Sigma Fe$ was reproduced for melt inclusions by our XANES method.

The methodology was then applied to determining the $Fe^{3+}/\Sigma Fe$ ratio of komatiite melt inclusions. Komatiites are rare, mantle-derived melts (restricted to the Archaean, with a few exceptions) that are characterized by MgO contents >18 wt%, and require a very high degree of partial mantle melting (up to 50%) in comparison with, for example, MORB (10–20%). Two models have been proposed to explain their origin: the plume, or 'hot-melting', model, involving decompression melting of a mantle source up to 500 °C hotter than today[1–3]; and the 'wet-melting' model, in which komatiites are Archaean analogues of modern subduction-related magmas with a mantle temperature only 100 °C hotter than today[4,5].

It should be possible to distinguish between the two models if well-preserved products of original komatiite melt were available. Unfortunately, most komatiites have been extensively altered as a result of their age. However, unusually fresh komatiite lava flows have been found within the Archaean Belingwe belt, Zimbabwe, which contain olivine phenocrysts ($Fo_{89.0–93.5}$) that have preserved inclusions of the original melt[6,7,23]. We heated the inclusions, which at room temperature have recrystallized into an aggregate of olivine, pyroxene and interstitial glass, to 1,300 °C in 30 s and quenched them to give a homogeneous glass (Fig. 3). The composition of the glass differs from that of the originally trapped melt, owing to crystallization of olivine on the inclusion walls that is not re-dissolved on heating[24,25] and post-entrapment equilibration with the host olivine[7,25]. Both of these effects will shift the $Fe^{3+}/\Sigma Fe$ ratio of the glass to higher values, and the values determined here thus represent upper limits. The inclusions were prepared as free-standing sections (which are also ideal for the determination of water contents by infrared spectroscopy).

The pre-edge region of the XANES spectrum of a komatiite melt inclusion is shown in Fig. 1b. It is apparent, in relation to MORB, that the inclusion is reduced. Using the calibration curve in Fig. 2, the average $Fe^{3+}/\Sigma Fe$ value of four komatiite inclusions was determined to be 0.10 ± 0.02 (the individual values were 0.10 ± 0.01, 0.11 ± 0.03, 0.08 ± 0.01 and 0.10 ± 0.01).

Fertile mantle peridotite contains 0.3 wt% Fe_2O_3, implying a $Fe^{3+}/\Sigma Fe$ value of 0.035 ± 0.005 for a source with 6.3 wt% ΣFe (refs 26, 27). Assuming bulk melt–residue partition coefficients of 1 for FeO and 0.1 for Fe_2O_3 (ref. 26), 15% batch melting of peridotite, which is appropriate for the genesis of primitive MORB, should result in a melt with $Fe^{3+}/\Sigma Fe \approx 0.13$. This is in agreement with what is routinely observed, demonstrating that MORBs reliably reflect the oxidation state of their sources. Higher degrees of partial melting lower the $Fe^{3+}/\Sigma Fe$ value of the magma by dilution; with the same partition coefficients, the $Fe^{3+}/\Sigma Fe$ range of 0.08–0.12 found here for the komatiite melt inclusions would correspond to 16–33% partial melting. Even greater degrees of partial melting are inferred if, as is probable, the partition coefficient of Fe_2O_3 decreases with increasing melting as pyroxenes, the main crystalline hosts of this component, are progressively eliminated from the residue[28]. The oxidation state of the Belingwe komatiite source is therefore, within uncertainty, the same as the source of modern MORB, in agreement with that deduced from V/Sc systematics[29]. By contrast, arc peridotites indicate that hydrated

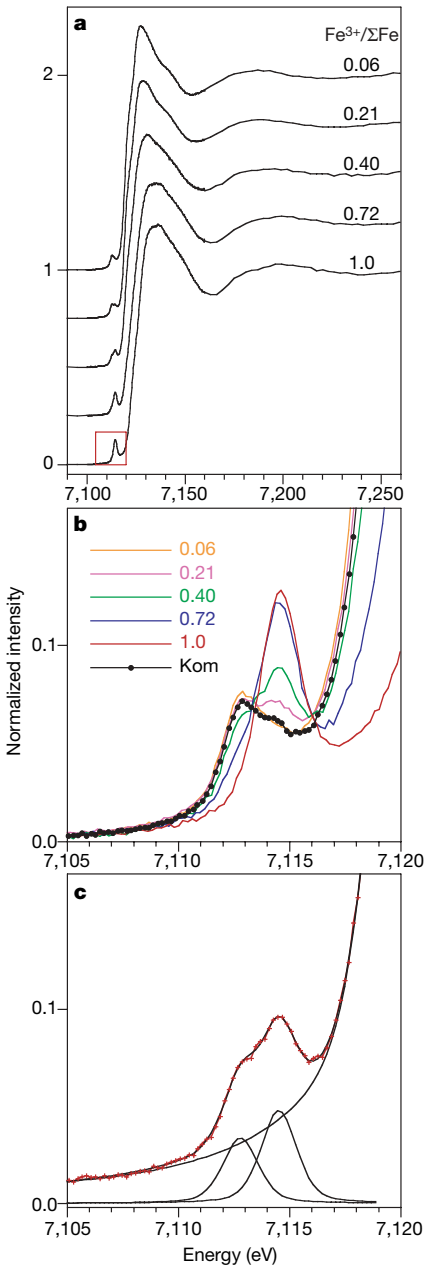

Figure 1 | Iron K-edge XANES spectra of quenched silicate melts. **a**, Spectra of synthetic MORB glass standards with the $Fe^{3+}/\Sigma Fe$ values indicated. Spectra have been offset for clarity. **b**, XANES pre-edge region, indicated by the box in **a**, showing the $1s \rightarrow 3d$ transition of both the MORB standards and a natural komatiite melt inclusion (Kom). **c**, Fit to the pre-edge of the MORB standard with $Fe^{3+}/\Sigma Fe = 0.40$, showing the data (symbols), the baseline and the pseudo-Voigt components.

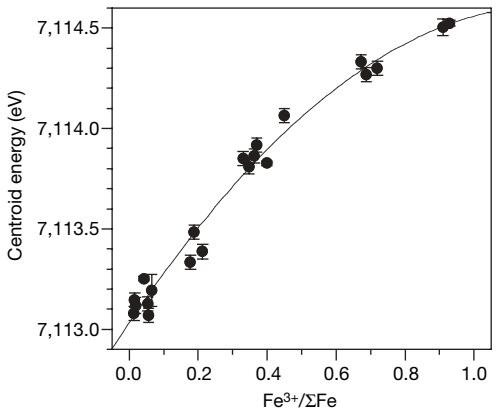

Figure 2 | Calibration curve for determining $Fe^{3+}/\Sigma Fe$ from the XANES pre-edge centroid energy. The curve is derived from a second-order polynomial fit to data for MORB, tholeiite, pantellerite and andesite standards; error bars, 1 s.d., determined from replicate measurements.

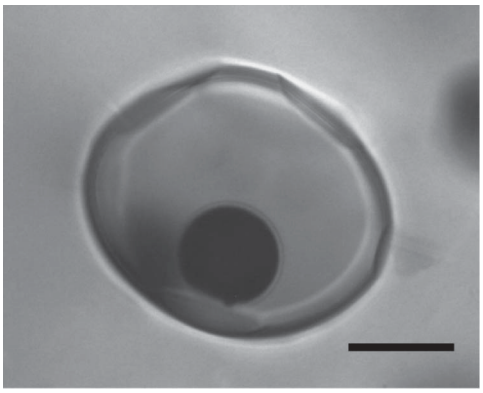

Figure 3 | Optical image of an olivine-hosted melt inclusion (after heating) from a komatiite of the Belingwe belt, Zimbabwe. The inclusion comprises quenched melt (glass) and a dark 'shrinkage bubble'; scale bar, 20 μm.

mantle is much more oxidized[30], leading to the characteristic highly oxidized signature of subduction-related magmas[8].

The measured water contents of the komatiite inclusions range from 0.18 to 0.26 wt% (ref. 7), which is far less than the 3 to 5 wt% required by the wet-melting model. However, melt inclusions can change their water contents after entrapment, through loss by diffusion of H_2 or water (ref. 24). Loss of water results in the formation of haloes of tiny fluid inclusions and recrystallized host mineral rims[31]. No such structures were observed in the komatiite samples studied. The most probable process, however, involves reduction of water to H_2, which may then diffuse rapidly out of the sample. Such reduction must result in the concomitant oxidation of another species, with iron being the only polyvalent element present in sufficient abundance to form the other half of the redox pair; that is, $H_2O_{(melt)} + 2FeO_{(melt)} = H_{2(gas)} + Fe_2O_{3(melt)}$. Loss of water by H_2 diffusion is therefore associated with an increase in $Fe^{3+}/\Sigma Fe$, and complete oxidation of an inclusion with 12 wt% FeO would be expected (that is, $Fe^{3+}/\Sigma Fe = 1$) for the loss of only 1.5 wt% water.

The komatiite melt inclusions therefore show no evidence for the loss of water either directly or by reduction and diffusion of H_2, and the measured water contents are likely to be those of the original melt. These results are consistent with the 'anomalously hot mantle' model for the formation of the Belingwe komatiite. The results also show that despite the higher temperature of the komatiite source, its oxidation state was similar to that of present-day mantle, which rules out significant interactions with either the core (more reduced) or crustal material (more oxidized); it also argues against increases in the oxidation state of the mantle over geological time, contrary to some hypotheses (ref. 32 and references therein). The XANES technique is ideally suited to determining the $Fe^{3+}/\Sigma Fe$ ratio of melt inclusions, as it provides the necessary spatial resolution, the samples are isotropic and, hence, orientation independent, and compositionally matched standards can be prepared using the methods of experimental petrology. The method opens up the possibility for the routine determination of redox state in geological samples on the same analytical scale as is currently achievable for major elements by the electron microprobe and trace elements by ion microprobe and laser-ablation mass spectrometry.

METHODS SUMMARY

Synthetic glass standards were prepared by equilibrating reagent-grade oxide mixes in a 1-atm gas mixing furnace at 1,400 °C, using $CO/CO_2/O_2$ to control f_{O_2} at log values relative to the nickel–nickel-oxide buffer (NNO) of −5, −2, +1, +3 and +6, followed by quenching in water[18,19]. Samples were also prepared at NNO + 11 by equilibrating with PtO_2 in a sealed platinum capsule at 10 kbar and 1,400 °C using a piston–cylinder apparatus. The $Fe^{3+}/\Sigma Fe$ ratio of each glass can be estimated using an empirical expression that relates Fe^{3+}/Fe^{2+} to f_{O_2}, temperature, pressure and composition[33]. In this way, standards of any melt composition with any $Fe^{3+}/\Sigma Fe$ ratio can be obtained. Glasses with a pantellerite composition were prepared by equilibrating natural material in gas-mixing experiments; the $Fe^{3+}/\Sigma Fe$ ratios of these samples were determined by redox titration. All standards were thinned to produce doubly polished, free-standing sections with a thickness of 50–100 μm, which is close to the 1/e absorption path length of iron K-edge X-rays.

Iron K-edge XANES spectra were recorded at beamline 13-ID-C, GeoSoilEnviroCARS (GSECARS, University of Chicago), of the Advanced Photon Source (Argonne National Laboratory, USA). Owing to the large penetration depth of the analysis beam, it was necessary to consider the entire beam trajectory through the sample and the potential for excitation of the host olivine ($Mg_{1.8}Fe_{0.2}SiO_4$). This was avoided by preparing inclusions such that they are exposed on both sides of the section and orienting the sample normal to the beam, which was focused to a spot with a diameter of ~5 μm.

Full Methods and any associated references are available in the online version of the paper at www.nature.com/nature.

Received 9 March; accepted 26 August 2008.

1. Green, D. H. Genesis of Archean peridotitic magmas and constraints on Archean geothermal gradients and tectonics. *Geology* **3,** 15–18 (1975).
2. Nisbet, E. G., Cheadle, M. J., Arndt, N. T. & Bickle, M. J. Constraining the potential temperature of the Archean mantle - a review of the evidence from komatiites. *Lithos* **30,** 291–307 (1993).
3. Arndt, N. *et al.* Were komatiites wet? *Geology* **26,** 739–742 (1998).
4. Allegre, C. J. in *Komatiites* (eds Arndt, N. T. & Nisbet, E. G.) 495–500 (Springer, 1982).
5. Parman, S. W., Grove, T. L. & Dann, J. C. The production of Barberton komatiites in an Archean subduction zone. *Geophys. Res. Lett.* **28,** 2513–2516 (2001).
6. Nisbet, E. G. *et al.* Uniquely fresh 2.7 Ga komatiites from the Belingwe greenstone-belt, Zimbabwe. *Geology* **15,** 1147–1150 (1987).
7. Danyushevsky, L. V., Gee, M. A. M., Nisbet, E. G. & Cheadle, M. J. Olivine-hosted melt inclusions in Belingwe komatiites: implications for cooling history, parental magma composition and its H_2O content. *Geochim. Cosmochim. Acta* **66** (Suppl. 1), A168 (2002).
8. Carmichael, I. S. E. The redox states of basic and silicic magmas: a reflection of their source region. *Contrib. Mineral. Petrol.* **106,** 129–141 (1991).
9. Self, S., Thordarson, T. & Widdowson, M. Gas fluxes from flood basalt eruptions. *Elements* **1,** 283–287 (2005).
10. Christie, D. M., Carmichael, I. S. E. & Langmuir, C. H. Oxidation states of mid-ocean ridge basalt glasses. *Earth Planet. Sci. Lett.* **79,** 397–411 (1986).
11. Bezos, A. & Humler, E. The $Fe^{3+}/\Sigma Fe$ ratios of MORB glasses and their implications for mantle melting. *Geochim. Cosmochim. Acta* **69,** 711–725 (2005).
12. Jayasuriya, K. D., O'Neill, H. St C., Berry, A. J. & Campbell, S. J. A Mössbauer study of the oxidation state of iron in silicate melts. *Am. Mineral.* **89,** 1597–1609 (2004).
13. Garvie, L. A. J. & Buseck, P. R. Ratios of ferrous to ferric iron from nanometre-sized areas in minerals. *Nature* **396,** 667–670 (1998).
14. Fialin, M., Bézos, A., Wagner, C., Magnien, V. & Humler, E. Quantitative electron microprobe analysis of $Fe^{3+}/\Sigma Fe$: basic concepts and experimental protocol for glasses. *Am. Mineral.* **89,** 654–662 (2004).
15. Delaney, J. S., Dyar, M. D., Sutton, S. R. & Bajt, S. Redox ratios with relevant resolution: solving an old problem by using the synchrotron microXANES probe. *Geology* **26,** 139–142 (1998).
16. Dyar, M. D., Delaney, J. S. & Sutton, S. R. Fe XANES spectra of iron-rich micas. *Eur. J. Mineral.* **13,** 1079–1098 (2001).
17. Bonnin-Mosbah, M. *et al.* Iron oxidation states in silicate glass fragments and glass inclusions with a XANES micro-probe. *J. Non-Cryst. Solids* **288,** 103–113 (2001).
18. Berry, A. J., O'Neill, H. St C., Jayasuriya, K. D., Campbell, S. J. & Foran, G. J. XANES calibrations for the oxidation state of iron in a silicate glass. *Am. Mineral.* **88,** 967–977 (2003).
19. Berry, A. J. & O'Neill, H. St C. A XANES determination of the oxidation state of chromium in silicate glasses. *Am. Mineral.* **89,** 790–798 (2004).
20. Westre, T. E. *et al.* A multiplet analysis of Fe K-edge 1s→3d pre-edge features of iron complexes. *J. Am. Chem. Soc.* **119,** 6297–6314 (1997).
21. Wilke, M., Farges, F., Petit, P.-E., Brown, G. E. Jr & Martin, F. Oxidation state and coordination of Fe in minerals: an Fe *K*-XANES spectroscopic study. *Am. Mineral.* **86,** 714–730 (2001).
22. Wilke, M., Partzsch, G. M., Bernhardt, R. & Lattar, D. Determination of the iron oxidation state in basaltic glasses using XANES at the K-edge. *Chem. Geol.* **213,** 71–87 (2004).
23. McDonough, W. F. & Ireland, T. R. The intraplate origin of komatiites inferred from trace elements in glass inclusions. *Nature* **365,** 432–434 (1993).
24. Danyushevsky, L. V., McNeill, A. W. & Sobolev, A. V. Experimental and petrological studies of melt inclusions in phenocrysts from mantle-derived magmas: an overview of techniques, advantages and complications. *Chem. Geol.* **183,** 5–24 (2002).
25. Danyushevsky, L. V., Sokolov, S. & Falloon, T. J. Melt inclusions in olivine phenocrysts: using diffusive re-equilibration to determine the cooling history of a crystal, with implications for the origin of olivine-phyric volcanic rocks. *J. Petrol.* **43,** 1651–1671 (2002).

26. Canil, D. *et al.* Ferric iron in peridotites and mantle oxidation states. *Earth Planet. Sci. Lett.* **123,** 205–220 (1994).
27. Palme, H. & O'Neill, H. St C. in *The Mantle and Core* (ed. Carlson, R. W.) 1–38 (Treatise on Geochemistry 2, Elsevier, 2003).
28. Canil, D. & O'Neill, H. St C. Distribution of ferric iron in some upper-mantle assemblages. *J. Petrol.* **37,** 609–635 (1996).
29. Canil, D. Vanadium partitioning and the oxidation state of Archaean komatiite magmas. *Nature* **389,** 842–845 (1997).
30. Parkinson, I. J. & Arculus, R. J. The redox state of subduction zones: insights from arc-peridotites. *Chem. Geol.* **160,** 409–423 (1999).
31. Danyushevsky, L. V., Berry, A. J., O'Neill, H. St C., Newville, M. & Sutton, S. R. Fe^{3+}/Fe^{2+} of melt inclusions: implications for melt H_2O contents. *Geochim. Cosmochim. Acta* **71,** A200 (2007).
32. Galimov, E. M. Redox evolution of the Earth caused by a multistage formation of its core. *Earth Planet. Sci. Lett.* **233,** 263–276 (2005).
33. Kress, V. C. & Carmichael, I. S. E. The compressibility of silicate liquids containing Fe_2O_3 and the effect of composition, temperature, oxygen fugacity and pressure on their redox states. *Contrib. Mineral. Petrol.* **108,** 82–92 (1991).

Supplementary Information is linked to the online version of the paper at www.nature.com/nature.

Acknowledgements We thank D. R. Scott for sample preparation, N. Métrich for providing the pantellerite glass standards and G. J. Foran for assistance with XANES experiments at the Australian National Beamline Facility that provided the foundations for the present study. We also thank the Australian Research Council (DP0450252), the Access to Major Research Facilities Programme (funded by the Commonwealth of Australia) and the Natural Environment Research Council for financial support. GeoSoilEnviroCARS is supported by the US National Science Foundation (EAR-0622171) and the US Department of Energy (DE-FG02-94ER14466). Use of the Advanced Photon Source was supported by the US Department of Energy, Office of Science, Office of Basic Energy Sciences, under contract no. W-31-109-Eng-38.

Author Contributions A.J.B. and H.StC.O'N. prepared the synthetic samples and collected the XANES spectra, with assistance from M.N. and S.R.S. The natural samples were prepared and characterised by L.V.D., who identified the importance of determining $Fe^{3+}/\Sigma Fe$ in komatiite melt inclusions. A.J.B. interpreted the spectra and produced the manuscript with significant contributions from H.StC.O'N. and L.V.D.

Author Information Reprints and permissions information is available at www.nature.com/reprints. Correspondence and requests for materials should be addressed to A.J.B. (a.berry@imperial.ac.uk).

METHODS

For the acquisition of XANES spectra, samples were mounted on Kapton tape and viewed from behind (downstream) using a long-working-distance objective located on the beam axis, which was removed during spectral acquisition. The optics allowed the beam to be accurately positioned on selected parts of a sample. To be certain that fluorescence from the host olivine did not contribute to the iron spectrum, the Kα intensity of nickel was monitored; nickel is an order of magnitude more abundant in the olivine than the inclusion. The excitation energy was selected using a Si(111) double-crystal monochromator and focused with Kirkpatrick–Baez mirrors. The spectral resolution at the iron K edge is ~1.6 eV. Spectra were recorded from 7,050 to 7,300 eV using step sizes of 2 eV from 7,050 to 7,100 eV, 0.2 eV from 7,100 to 7,160 eV, and 3 eV above 7,160 eV, in both transmission (ion chamber detector) and fluorescence (16-element germanium array detector) modes, although only fluorescence spectra are reported here. Spectra recorded sequentially as a function of time were identical and there was no evidence of any beam-induced changes in oxidation state. An iron foil spectrum was simultaneously acquired using the transmitted beam, allowing the energy of every sample spectrum to be individually calibrated by defining the first-derivative peak of the iron foil spectrum to be 7,112.0 eV. The sloping baseline between 7,050 and 7,100 eV was fitted to a linear function and the spectra 'straightened' before normalization to the average fluorescence above 7,200 eV.

The MORB sample (WW10-113-16) was dredged from the southeast Indian ridge at 105.22° E, 48.75° S during the WW10 voyage of the RV *Melville* in 1995.